Adaptive Optics J Band Imaging Polarimetry Observations of the Circumbinary Disk around UY Aurigae

Daniel E. Potter, Laird M. Close, François Roddier, Claude Roddier, J. E. Graves, Malcolm Northcott

University of Hawaii, Manoa, Institute for Astronomy, Honolulu, HI 96822

Abstract. We have obtained J band (1.2 μm) polarimetry observations of the circumbinary disk around UY Aurigae with the University of Hawaii 36 element adaptive optics instrument, Hokupa'a, at the 3.6 m CFHT. The deep (120 min), high resolution (0.15") polarization map reveals a centrosymmetric polarization signature from the light scattered off the circumbinary dust disk which is ~10^6 times fainter than the stars in the binary system. PLUCY deconvolution is shown to successfully remove the wings of the unpolarized stellar PSF which contaminates the polarization signal of the disk. The first measurements of the polarization (~1.5%) of the two individual stellar components of UY Aur are reported as well.

1.0 Introduction

Near infrared observations of the circumstellar disks around T-tauri stars are difficult due to the close proximity of these disks to their bright central star(s). Consequently, only a handful of circumstellar disks around T-Tauri stars have been resolved in their scattered light (see McCaughrean, Stapelfeldt, & Close 1998). There is very limited information on the composition and size distribution of the cool dust in these disks. However, this information is crucial to the understanding of how planets form. The degree of density inhomogeneity in these disks which is vital to the understanding of the possible mechanisms of planet formation is also a poorly understood characteristic. Already there is observational evidence for clumps or structure of material in the UY Aur disk (Close et al. 1998). Studying the scattered light from the dust in these disks with high-resolution infrared imaging and polarimetry, coupled with the knowledge of how dust scatters light allows for basic statements to be made regarding the nature of the dust population in these disks.

Adaptive optics instrumentation, which provide high angular resolution, high dynamic range, stable PSF images, is now available to carry out these studies for objects with large circumbinary disks. The circumbinary disk (one large disk around both stars) of UY Aur is well suited for adaptive optics as it is of considerable separation (~2”) from the central star (UY Aur A) which is bright enough to be an adequate wavefront beacon (V~12). The circumbinary CO gas disk around UY Aur was first resolved in a high resolution millimeter survey of T-Tauri stars with infrared excesses (Dutrey et al. 96) and then found to be in Keplerian rotation by Duvert et al. (1998). The disk was then resolved in the infrared at high resolution with adaptive optics by Close et al. (1998).

In this paper we discuss the data reduction techniques used to produce high resolution, high dynamic range polarization maps with adaptive optics images using the polarization observations of the circumbinary disk around UY Aurigae. The resulting polarization map of the disk shows a centrosymmetric pattern around the central binary pair. A comparison with a Mie single-scattering model of the disk provides convincing evidence that the scattered light is coming from a flattened (possibly flared) dust disk rather than from a spherical distribution of optically thin dust.

2.0 Observations and Reductions

Observations were obtained with the University of Hawaii 36 element curvature wavefront sensing adaptive optics instrument, Hokupa’a (Graves et al. 1998; see http://www.ifa.hawaii.edu/ao), mounted on the 3.6m Canada-France-Hawaii telescope (CFHT). The night of the observing (November 15, 1997) was photometric and the natural seeing was 0.7” FWHM in the visible. The exposures were taken with the 1024x1024 HgCdTe near infrared camera, QUIRC (Hodapp et al. 1996) with a 0.0365”/pixel platescale. This system produced diffraction-limited images (Strehl~0.2, FWHM~0.09” at J) when a V~12 guide star (UY Aur A) was used as the wavefront beacon.

The linear polarization measurements were obtained with four successive exposures per dither position through a standard J-band filter (1.25 μm) in series with an IR-optimized half-wave plate with rotations of 22.5^{o} between exposure.

These 22.5^{o} rotations effectively rotate the linear polarization vector in steps of 45^{o} for a cooled wire grid analyzer placed inside the IR camera. Ten minute exposures for each of the four polarimetry angles (0^{o},45^{o},90^{o},135^{o}) were taken for all three dither positions totalling 120 minutes (10 min x 4 x 3) of exposure time. These long exposures saturated the central core of each of the stellar components revealing the very faint scattered light of the previously observed circumbinary disk (Close et al. 1998). Three shorter, 10 sec, unsaturated exposures per filter position where also taken at each of the three dither positions totalling 360 seconds (10 sec x 3 x 4 x 3) to measure the polarization of the two stellar components of UY Aur. Polarimetry for the calibration standard Elias 3-19 (Whittet et al. 1992) was performed through the same optical path as the above observations. Three one second exposures were taken at each of the four half waveplate positions for three dither positions (3x3x4 exposures in total). These exposures were taken with the AO system turned off in order to accumulate a larger number of counts on the detector before saturating the center pixels of the PSF.

All the images were sky subtracted and flat fielded in the standard fashion. The same sky and flat field were used for each image sharing common exposure times, so each of the four different polarization images in each set were reduced with the same flat and sky frames. All of the polarization values in this paper are obtained using the standard Stokes equations applied to polarization images with four steps of 45^{o} rotations.

2.1 Polarization Calibration star

Aperture photometry (5” radius) was performed on the multiple exposures of the polarization calibration star Elias 3-19. The normalized Q and U values obtained from the aperture photometry were medianed. The polarization intensity of Elias 3-19 was found to be 2.5±1.5% (See Table # 1). This is consistent with the 3.1% polarization determined for the standard (Whittet, 1992). The angle of the polarization agreed with the angle calibration derived by Close et al. (1997) of the R Mon NGC2261 reflection nebula.

2.2 Short exposures of UY Aur

The series of 10 second exposures were sky subtracted and flat fielded with the off-object sky flat. The images taken at different dither positions but sharing the same polarimetry positions were aligned using cross-correlation techniques applied to the unsaturated UY Aur A and B components and were then median combined. Aperture photometry was then carried out on each of the median combined images. The results are shown in Table 1. The stars themselves are currently not significantly polarized. However, Menard & Bastien (1986) observed a “polarization flare”(~8%) from the unresolved UY Aur system. UY Aur does not appear to be currently flaring.

The low stellar polarization observed is not surprising for UY Aur A since it has a low extinction (A_V~1), and therefore presumably less intervening circumstellar dust. However, the much more reddened B component, A_V~9.2 (Herbst, Koresko, & Leinert 1995) has the same polarization as A. This result suggests the dust grains responsible for the observed reddening have no charge dipole (spherical) or if they have a dipole they are not aligned.

Table 1: Point Source Polarimetry

Star	Polarization	Pol. Angle	A_V*
UY Aur A	1.5%±0.7%	42.0^{o}±10^{o}	1.04
UY Aur B	1.5%±0.7%	-4.1^{o}±13^{o}	9.2
Elias 3-19 (Obs.)	2.5%±1.5%	-1.8^{o}±15^{o}	N.A.
Elias 3-19 (Std.)**	3.06%±0.05%	36^{o}±1^{o}	N.A.

* from Close et al. 1998
** from Whittet et. al. 1992

2.3 Deep Exposures of UY Aur

The three dither positions of the 600 sec data were aligned using cross correlation techniques applied to an unsaturated field star (~13” N and 10” E from UY Aur A) common to each dither position. The polarization intensities and vector angles were then obtained using the LINPOL IRAF routine. The resulting three U and Q images from the three dither positions were then median combined. The final medianed polarization map revealed a centrosymmetric pattern in only the brightest area of the circumbinary disk (~10^5 times fainter than the stellar components) with the rest of the disk's polarization signal dominated by the unpolarized light from the central stars' PSF wings.

2.3.1 PSF Removal

The IRAF PLUCY deconvolution algorithm (Hook et al. 1996) was used in an attempt to reduce the contamination of the polarization signal of the faint (~10^6 times fainter than the stellar components) circumbinary disk by the PSF wings produced by the bright components. A very high dynamic range ($2x10^6$) PSF was developed through a MULTIACCUM set of exposures (7x3sec+12x15sec+10x60sec) totalling 13.35 minutes on a nearby SAO star of similar brightness and identical airmass. This high contrast PSF was used to deconvolve all twelve of the 600 sec polarization exposures from the three dither positions. After a light treatment of 30 iterations of PLUCY, the signal to noise of the disk improved significantly as the stellar PSF wings were removed. The final U and Q maps were then obtained from the median of the deconvolved maps. Hence, a greatly improved signal to noise centrosymmetric pattern was restored in the final polarization map.

Small exposure to exposure variations in the uncompensated adaptive optics halo around the PSF prohibit an accurate measure of polarization values within ~1" of the bright stars. These regions with poor PSF stability and where there were saturated pixels inside 1", have been masked out. The resulting polarization map is overlaid upon the (Close et al. 1998) PLUCY deconvolved J-band image in Figure 1.

3.0 Results

The observed polarization signature of UY Aur's circumbinary disk exhibits a number of characteristics. Apparent is a peak in polarization intensity (at position angle, PA=130^o and -40^o). These peaks correspond close to where the predicted 90^o scattering angle (to our line of sight) is located for a disk with a semi-major axis PA of 135^o and inclined at 42^o (see Close et al. 1998). A decrease in polarization intensity on either side of the 90^o scattering angle around PA~130^o (see Figure 2) is also observed.

The average polarization increases radially by ~7% per arcsec. Also, the center of the centrosymmetric pattern is observed to vary on the different sides of the disk. The SE portion of the disk is centered on UY Aur B with the opposite side centered more on the systems' photo-center in-between UY Aur A and B. However, all the centrosymmetric vectors are consistent with a center within 0.5" of the binary photocenter.

3.1 Model Comparison

A Mie scattering code (see Bohren and Huffman 1983 for more detail about the exact Mie solution) was developed for circumbinary disks in Close et al. (1998). The model calculates the relative stokes parameters versus scattering angle projected onto a disk of given inclination angle. To model the dust grains in the UY Aur disk we used the best fit from χ^2 minimization routines which found the maximum dust grain size and the power-law index of the grain size distribution from the front-back ratios of J, H, and K band observations of the UY Aur circumbinary disk (Close et al. 1998). The resulting values give a steep number density power law, $N(a)\alpha a^{-4.7}$, with a maximum grain radius of a_{max}~0.6 μm. On the whole this is consistent with the general ISM grains of Mathis and Whiffen (1992).

We compared of our observed polarization intensity versus position angle to that produced by the model pictured in Figure 2 and to that expected by an optically thin spherically symmetric distribution of dust (no position angle dependence on polarization intensity). The observed peak polarizations at position angles corresponding to the 90^o scattering angle and the observed polarization intensity decrease away from this position angle favors the flattened disk model rather than the spherical envelope of optically thin dust scenario.

3.1.1 Nature of the Radial Increase in Polarization

Our Mie single-scattering disk model is not equipped to predict or interpret radial variations of the polarization signal with changes in optical depth. However, the polarization value considering multiple scattering events has been modeled with Monte Carlo simulations by a number of efforts (c.f. Wood et al. 1996) which show an increase of polarization with radius in the case of an optically thick disk which has a decreasing optical depth with increasing radius.

However it is uncertain how much of the polarization signal seen from the disk is damaged by the unpolarized light from the stellar PSFs. It is noted that the polarization values where there is high confidence of real signal increase with radial distance from the central source, which follows with the decrease in PSF light. In the optimistic case where the PSF is degrading the signal of the disk in all of the deconvolved images in exactly the same manner, then the resulting decrease in polarization intensity would follow the relation:

$$\frac{Pobs}{Ptrue} = \frac{1}{1+2f}$$

If I_{psf}=fI_{disk}.

The factor, f would decrease with increasing radius from the central stars as the wings of the PSF diminish. Random errors associated with the changes of the PSF from frame to frame would also have the same radial effect on the polarization upon taking the vector median of three dither positions.

Because of the uncertainty in how much the PSF is contaminating the signal of the scattered light from the disk, we can offer only a qualitatively description of the benefit of The PLUCY algorithm in that it removes a significant portion of the wings of the central stars while preserving the light from the disk. In the case of the UY Aur circumbinary disk, the centro-symmetric pattern was quickly enhanced with the light use of the PLUCY algorithm. This deconvolution effort was successful due to the incredible stability and consistency of the PSF produced by Hokupa'a. However, it is still unclear how to quantify the effects that the PLUCY deconvolution procedure has on the polarization vectors and what iteration number is optimal for polarization purposes. This number will vary upon the raw signal to noise which is not constant around the disk. This effort would benefit from a more advanced deconvolution procedure.

We know of no processing technique which would produce a centro-symmetric pattern and it is highly unlikely that the enhanced pattern we see after the PLUCY deconvolution is by chance. Thus it seems that deconvolution of adaptive optics polarization images offers promise for performing high resolution polarimetry on faint surface brightness material close to bright sources. The issue of how to quantify the effects of deconvolution on polarization data is left for future efforts.

4.0 Conclusions

We have produced the first high-contrast, high-resolution polarimetry map of the circumbinary disk around UY Aurigae. This map supports the previously introduced scenario (Close et al. 1998) that the extended IR surface brightness observed around UY Aur is from a flattened dust disk (rather than a spherical envelope of dust) with a relatively large number of small grains.

In the process of reduction we found the PLUCY algorithm successfully removed a significant portion of the PSF wings of the central stars while preserving the light from the circumbinary disk. Hence, with the light use of the PLUCY algorithm, a strong centrosymmetric pattern is quickly restored. This deconvolution effort was successful due to the excellent stability and consistency of the PSF produced by Hokupa'a. Thus, this effort demonstrates the potential use of ground based adaptive optics polarimetry as a powerful tool for probing the dust grain population and geometry in circumstellar disks.

The University of Hawaii 36 element curvature adaptive optics instrument, Hokupa'a, was developed under NSF grant AST96-18852. This work could not have been carried out without the support of NSF grant AST97-31576.

References

Bohren, C.F., & Huffman, D.R. 1983, Absorption and Scattering of Light by Small Particles (New York: Wiley & Sons)
Close, L. M., et al. 1998, ApJ, 499, 883
Close, L. M., et al. 1997 ApJ, 489, 210
Dutrey, A., Guilloteau, S., Duvert, G., Prato, L., Simon, M., Schuster, K., & Menard, F. 1996, A&A, 309, 493
Duvert, G., et al. 1998, A&A, 332, 867
Graves, J.E, Northcott, M., Roddier, F., Roddier, C., Close, L.M., 1998, Proc. SPIE, 3353, in press
Herbst,T.M., Koresko, C.D., & Leinert, C. 1995, ApJ, 452, 736
Hodapp, K.-W., et al. 1996, New Astron., 1, 177
Hook, R.N., Lucy, L. B., Stockton, A., & Ridgway, S. 1994, Two Channel Photometric Image Restoration, ST-ECF Newslett. 21, 16
Mathis, J.S. & Whiffen, G. 1989, ApJ, 341, 808
McCaughrean, M., Stapelfeldt, K., & Close, L.,M. Planets and Protostars IV, Santa Barbara, July 6-12, 1998
Menard, F. & Bastien, P., 1986, IAU Symp. 122, 133
Whittet, et al. 1992, ApJ 386, 562
Wood, K. J., Bjorkman, J.E., Whitney, B. A., & Code, A. D. 1996, ApJ, 461, 828

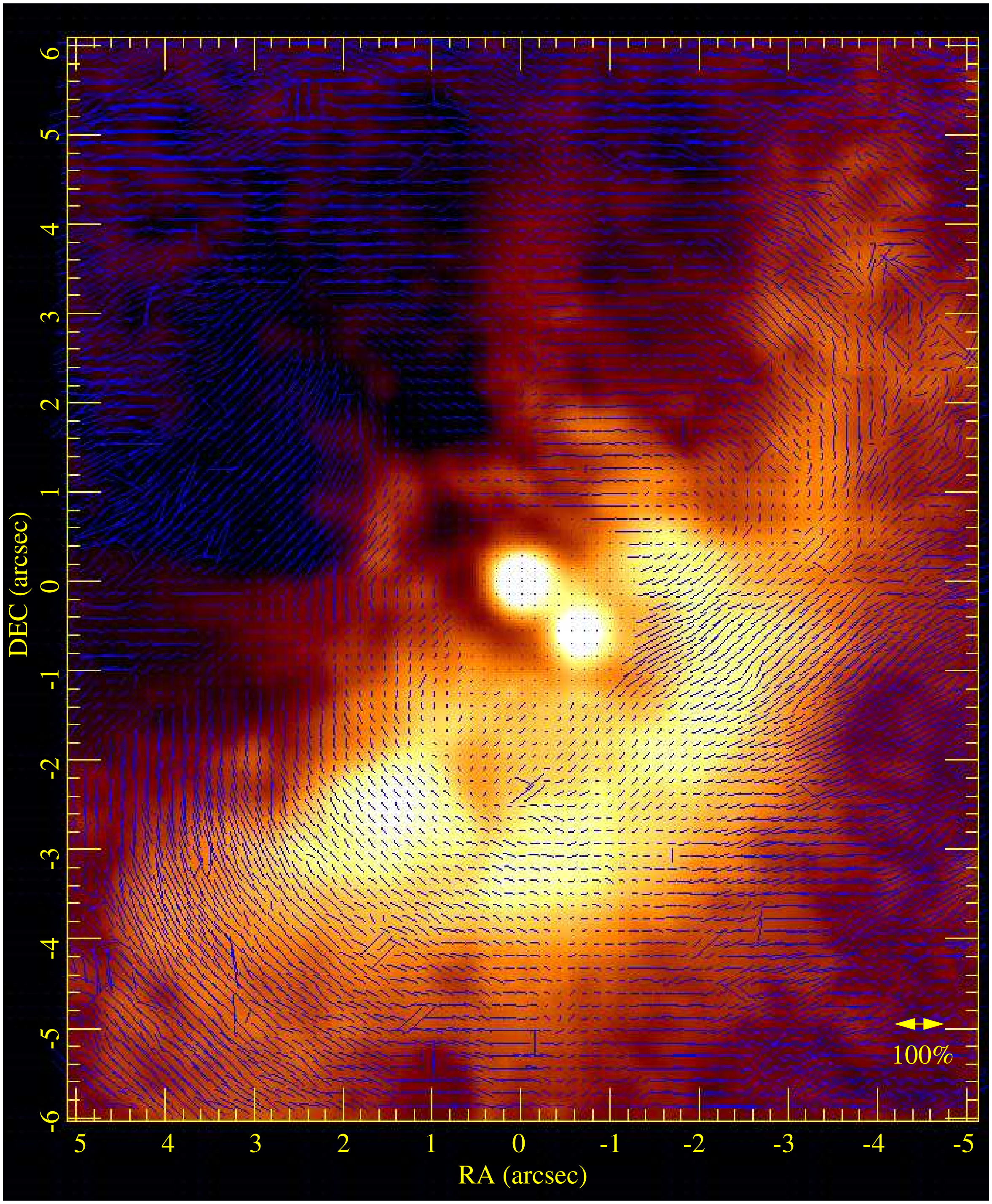

Fig. 1: The polarization vectors of the circumbinary disk around UY Aur are overlaid on the deconvolved logarithmic gray-scale image revealing the centrosymmetric pattern expected from scattered light. Bad pixels are not masked as well as the four regions of the spider arm diffraction spikes. However, the polarization vectors of the saturated, high stellar PSF noise region near the central stars (1.0" radius) have been masked. Position angle (PA) is 0^{o} to the North and increases to the East (90^{o}).

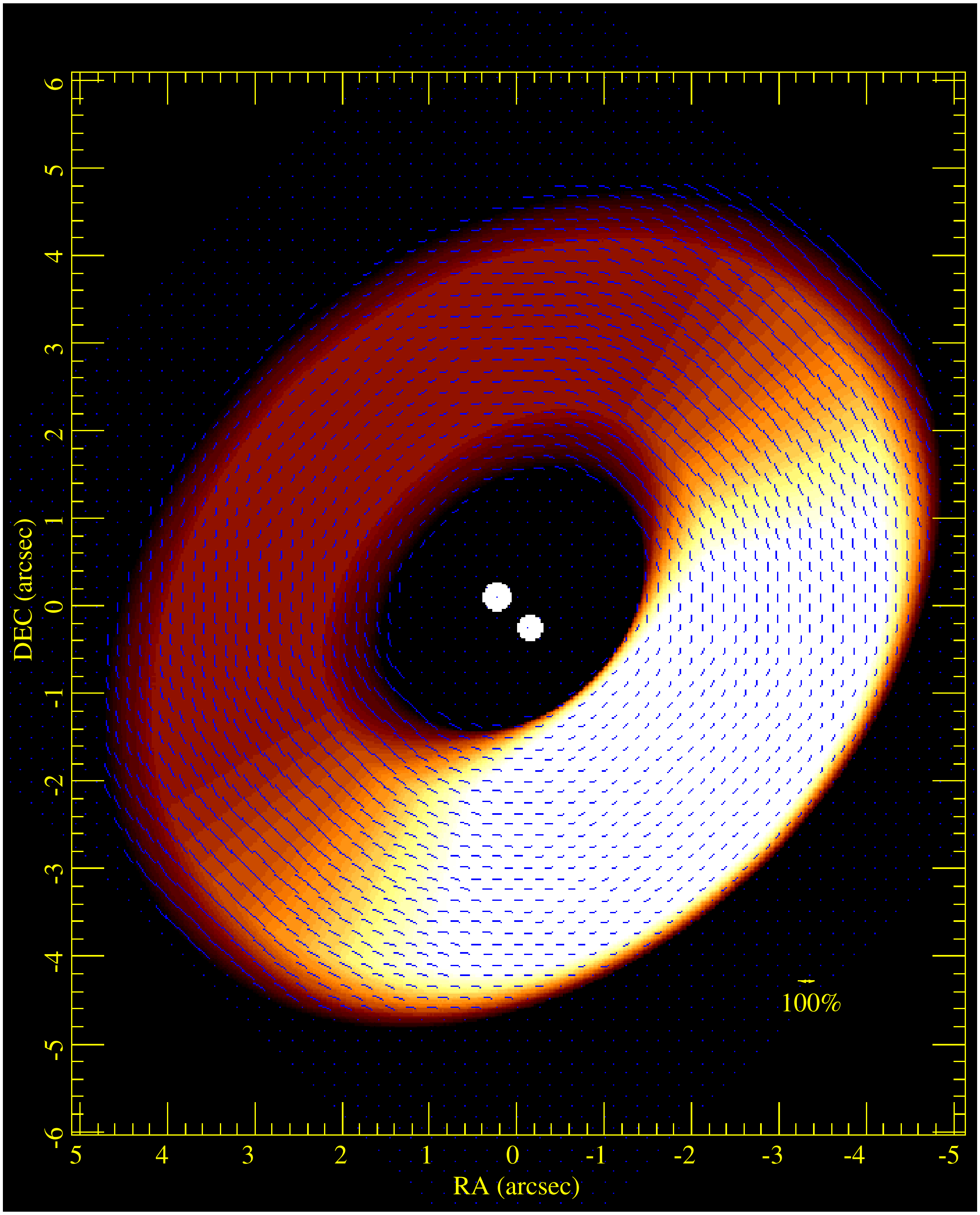

Fig. 2: A Mie single-scattering model of a flattened dust disk with a power law (-4.7) size distribution of dust grains which best fits the observed front/back ratio of intensity previously observed (Close et al. 1998). The disk is circular when viewed face-on, but is shown here inclined 42^{o}. The FRONT (or near) side of the disk is labeled (with the 48^{o} scattering angle to our line of sight in parentheses), as is the BACK (or far) side of the disk. The rise in polarization intensity at the sides of the disk where there is a 90^{o} scattering angle (PA=130^{o} and -40^{o}) is that expected from Rayleigh scattering off a flattened disk. This Rayleigh-like scattering is indicative of large numbers of small grains (<0.1 μm).

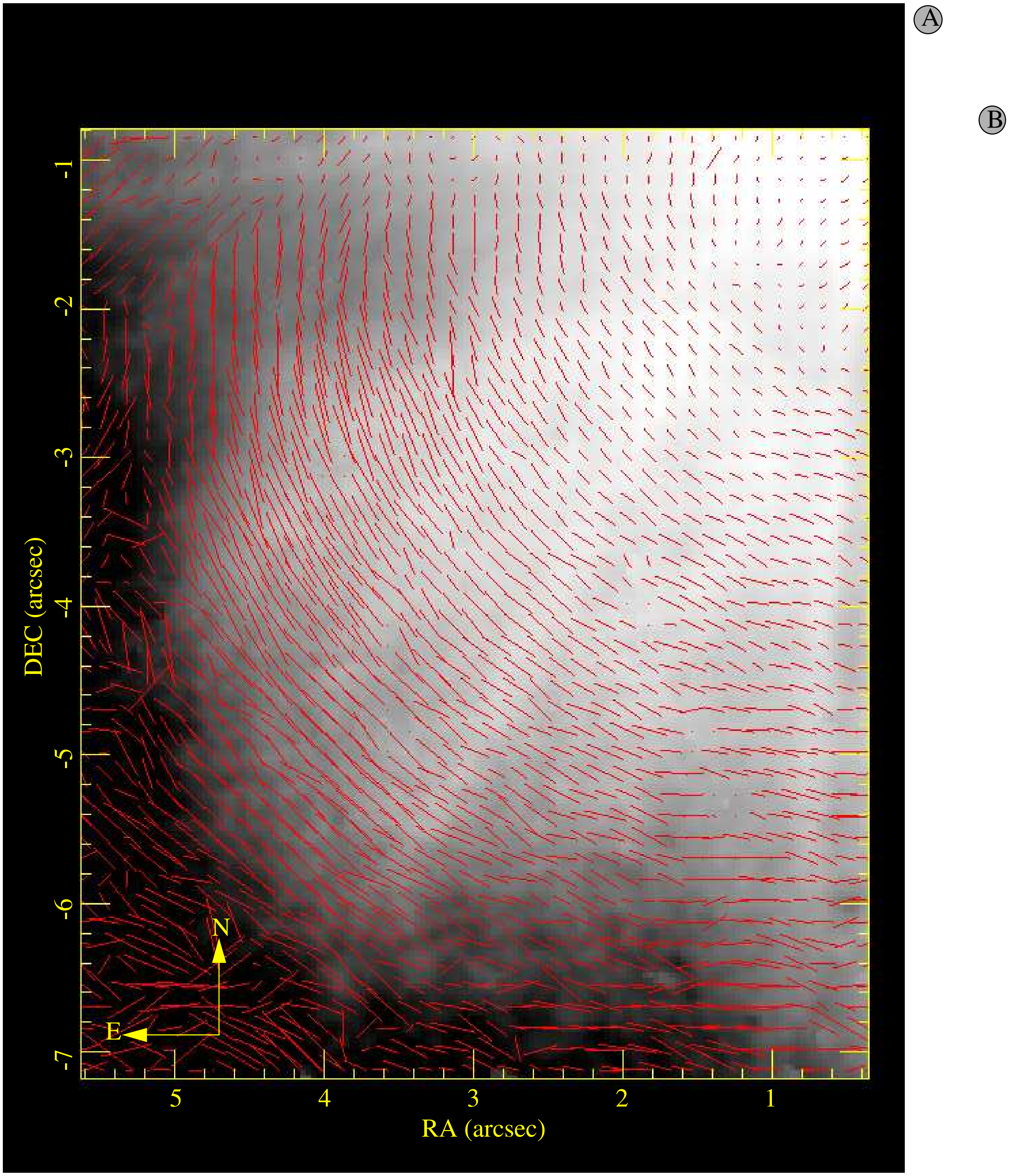

Fig. 3: Here is a detailed view centered on the SE clump of material shown in Figure 1. The peak polarization is observed at the 90^{o} scattering angle (PA~130^{o}) predicted by the Mie single-scattering dusty disk model. The model predicted decrease in polarization on either side of 90^{o} (PA~130^{o}) is also observed. Vectors tainted with bad pixels have been removed.